

IN-92-711
57828
0.36

ON REFLECTION OF ALFVÉN WAVES IN THE SOLAR WIND

M. Krogulec and Z. E. Musielak*
Center for Space Plasma and Aeronomic Research
The University of Alabama in Huntsville
Huntsville, AL 35899, U.S.A.

and

Institute for Theoretical Physics and Astrophysics
The University of Gdansk
Gdansk, 80952 Poland

S. T. Suess and R. L. Moore ✓
Space Science Laboratory
NASA Marshall Space Flight Center
Huntsville, AL 35812, U.S.A.

S. F. Nerney
NRC/NAS Senior Resident Research Associate
NASA Marshall Space Flight Center
Huntsville, AL 35812, U.S.A.

*also Department of Mechanical and Aerospace Engineering

(NASA-TM-110642) ON REFLECTION OF
ALFVEN WAVES IN THE SOLAR WIND
(NASA Marshall Space Flight
Center) 36 p

N95-30582

Unclas

1.

G3/92 0057828

ABSTRACT

We have revisited the problem of propagation of toroidal and linear Alfvén waves formulated by Heinemann and Olbert [1980] to compare WKB and non-WKB waves and their effects on the solar wind. They considered two solar wind models and showed that reflection is important for Alfvén waves with periods of the order of one day and longer, and that non-WKB Alfvén waves are no more effective in accelerating the solar wind than WKB waves. There are several recently published papers which seem to indicate that Alfvén waves with periods of the order of several minutes should be treated as non-WKB waves and that these non-WKB waves exert a stronger acceleration force than WKB waves. The purpose of this paper is to study the origin of these discrepancies by performing parametric studies of the behavior of the waves under a variety of different conditions. In addition, we want to investigate two problems that have not been addressed by Heinemann and Olbert, namely, calculate the efficiency of Alfvén wave reflection by using the reflection coefficient and identify the region of strongest wave reflection in different wind models. To achieve these goals, we investigated the influence of temperature, electron density distribution, wind velocity and magnetic field strength on the waves. The obtained results clearly demonstrate that Alfvén wave reflection is strongly model dependent and that the strongest reflection can be expected in models with the base temperatures higher than 10^6 K and with the base densities lower than $7 \times 10^7 \text{ cm}^{-3}$. In these models as well as in the models with lower temperatures and higher densities, Alfvén waves with periods as short as several minutes have negligible reflection so can be treated as WKB waves; however, for Alfvén waves with periods of the order of one hour or longer reflection is significant, requiring a non-WKB treatment. We also show that non-WKB, linear Alfvén waves are always less effective in accelerating the plasma than WKB Alfvén waves. Finally, it is evident from our results that the region of strongest wave reflection is usually located at the base of

the models, and hence that interpretation of wave reflection based solely on the reflection coefficient can be misleading.

INTRODUCTION

The existence and importance of Alfvén waves in the solar wind has been known and extensively studied since the first work on this subject by Belcher and Davis [1971] and Belcher [1971]. The main purpose of those studies was to understand the role played by Alfvén waves in the wind acceleration and their possible association with plasma fluctuations observed in the solar wind. To gain physical insight into these problems, one must consider the propagation of Alfvén waves in a highly inhomogeneous medium with a background flow. In general, the problem is difficult because Alfvén waves propagating in inhomogeneous media may be coupled to other magnetohydrodynamic (MHD) waves, and then rigorous treatment would require finding solutions to the full set of MHD equations. However, early papers on this subject by Ferraro [1954] and Ferraro and Plumpton [1958] have shown that under some simplifications, linear Alfvén waves can be fully separated from other MHD waves. An additional simplification that has been often used to describe the propagation of Alfvén waves in the solar wind is the WKB approximation, which is an appropriate procedure for waves with wavelengths shorter than local characteristic scales [e.g., Belcher 1971; Hollweg 1973; Belcher and Olbert 1975; and Jacques 1977, 1978]. The WKB approximation, however, has long been known to be incorrect for wavelengths of typical Alfvén waves observed in the solar wind. Therefore, Heinemann and Olbert [1980, hereafter H&O] proposed a new mathematical approach which is independent of the WKB assumption and is based on the full Alfvén wave equations derived for the wave velocity and magnetic field perturbations [see also Hollweg 1990, and Barnes 1992]. The idea that Alfvén waves propagating in solar and stellar atmospheres must often be treated as non-WKB waves has been recently confirmed by An et al. [1989, 1990], Barkhudarov [1991], Velli, Grappin and Mangeney [1991], Velli [1993] and Lou and Rosner [1993]. In addition, Moore et al. [1991] have used non-WKB Alfvén waves to explain heating in solar coronal holes.

The fact that Alfvén waves propagating in nonuniform atmospheres may become non-WKB waves and suffer strong reflection has been known for a number of years [e.g., Thomas, 1983; Campos, 1987; and references therein]. Several different methods have been developed to address this problem. First, some attempts have been made to obtain full analytical solutions to the derived Alfvén wave equations and to determine the height in the atmosphere where the reflection becomes dominant in the wave behavior. Obviously, the closed form solutions can only be found for very few special cases; one celebrated example is the propagation of Alfvén waves in a plane parallel isothermal atmosphere permeated by a uniform and vertical magnetic field [Ferraro and Plumpton, 1958]. In this model, the upward propagating Alfvén waves of *all* frequencies are reflected and they always become standing waves. Second, it has been suggested that in order to determine the region in the atmosphere where wave reflection is the most important, it is sufficient to calculate a local cutoff frequency, which is usually defined as a ratio of wave velocity to a characteristic scale height. Having obtained the local cutoff frequency, one may then find the height in the atmosphere at which the wave frequency is comparable to the cutoff [Rosner, Low and Holzer, 1986; Musielak, Fontenla and Moore, 1992] and this height will identify the region of strong wave reflection. Finally, numerical solutions to the Alfvén wave equation can be obtained and non-WKB effects can be studied in detail [see H&O, also Hollweg 1990, and references therein]. We shall use this approach because the method presented by H&O is both a comprehensive and elegant treatment of Alfvén wave propagation in the solar wind.

There are two main conclusions in H&O's paper: (1) Alfvén waves in the solar wind with periods of one day and more must be treated as non-WKB waves, but shorter period waves can be described as WKB waves; (2) Non-WKB Alfvén waves are no more effective in accelerating the solar wind than WKB Alfvén waves. The problem is that results recently obtained by Barkhudarov [1991], Moore et al. [1991], Velli et al. [1991] and Velli [1993] seem to be in contradiction with the H&O conclusions. In particular, the authors of the three latter papers clearly indicate that Alfvén waves with periods as short

as 5 – 20 minutes can be reflected in the solar corona and provide acceleration and heating in the solar wind. In addition, Barkhudarov and Velli claim to have shown that some non-WKB Alfvén waves are much more effective in accelerating the wind than WKB waves. It must be noted that most of these recent results have been obtained by using methods which differ from the H&O approach; i.e., Barkhudarov and Velli modified the basic set of H&O equations by introducing new sets of variables and using different renormalization factors. More importantly, slightly different coronal and wind model have been used for each calculation. Because H&O performed their calculations for only two solar wind models and because Alfvén wave reflection depends sensitively on the choice of parameters that specify the model, our primary goal in this paper is to extend the H&O results over much broader (but observationally plausible) ranges of coronal and solar wind parameters. In addition, we want to study the spatial distribution of wave reflection to find the location of region in the model where reflection is strongest and to calculate the global efficiency of wave reflection by using the reflection coefficient.

To achieve these goals, we have adopted the H&O approach and numerically solved their wave equations. Our first task was to confirm their analysis and results, which we have successfully done. Then we investigated the propagation and reflection of Alfvén waves in a broad spectrum of wind models constructed for different magnetic field strengths, temperatures, and densities. The necessity for such investigations becomes apparent from a superficial study of H&O. A clear statement of how reflection depends on the complete set of coronal parameters used in the H&O model would be an important addition to the understanding of Alfvén wave reflection in the solar corona. It is also of interest to calculate the dependence of the global reflection coefficient on wave frequency in different models and compare the results to those previously obtained by other authors. We have also found where in the models wave reflection is strongest and compared the acceleration force for WKB and non-WKB waves. We believe that our results are helpful in clarifying the role played by WKB and non-WKB Alfvén waves in the solar wind.

BASIC FORMULATION AND PREVIOUS RESULTS

In general, the problem of propagation of Alfvén waves in the solar wind is complicated because the waves are usually coupled to other MHD modes. However, as shown by H&O, the coupling can be neglected when linear, toroidal Alfvén waves are considered. These waves have only ϕ components in spherical polar coordinates and, according to H&O, they can be described by two new wave variables: $u = V_\phi + V_{A\phi}$ and $v = V_\phi - V_{A\phi}$, where V_ϕ and $V_{A\phi}$ represent the ϕ -component of the wave velocity and the Alfvén wave velocity, respectively. A model of steady state and axisymmetric solar wind flow is assumed for the background medium, with the poloidal Alfvén velocity being related to the poloidal flow velocity by

$$\mathbf{V}_A = +\eta^{1/2}\mathbf{V}, \quad (1)$$

where η is the ratio of local gas density ρ to the gas density ρ_a at the Alfvénic critical point, which is defined as a point in the solar wind at which $V = V_A$. Note that the Alfvénic critical density ρ_a is a given field line constant. Because the flow is aligned with the local magnetic field, H&O introduced the arc length, s , along a given field line and defined two new wave variables

$$f = \frac{1 - \eta^{1/2}}{\eta^{1/4}} u, \quad (2a)$$

$$g = \frac{1 + \eta^{1/2}}{\eta^{1/4}} v, \quad (2b)$$

which represent the inward (f) and outward (g) propagating waves. By using the above definitions and these approximations to the set of ideal MHD equations, H&O derived the following equations:

$$\left[\frac{\partial}{\partial t} + (V - V_A) \frac{\partial}{\partial s} \right] f = g(V - V_A) \frac{d\psi}{ds}, \quad (3a)$$

$$\left[\frac{\partial}{\partial t} + (V + V_A) \frac{\partial}{\partial s} \right] g = f(V + V_A) \frac{d\psi}{ds}, \quad (3b)$$

where $\psi = -\ln(R\eta^{1/4})$ with $R = r \sin \theta$ being a distance to the symmetry axis. Equations (3a, b) showed that the wave amplitudes f and g are coupled together through the density

gradient $d\psi/ds$ and that the propagation of outward (inward) waves is modified by the existence of inward (outward) waves; the latter results from wave reflection due to the local density gradient. Note that in the WKB approximation, gradients in the background medium do not affect the wave propagation and, therefore, the inward propagating waves are not present.

To reduce the set of derived partial differential Equations (3a, b) to ordinary differential equations, H&O assumed that both f and g are periodic functions of time and used Fourier transforms

$$f(s, t) = \bar{f}(s)e^{-i\omega t}, \quad g(s, t) = \bar{g}(s)e^{-i\omega t}, \quad (4)$$

where $\bar{f}(s)$ and $\bar{g}(s)$ are the Fourier amplitudes. Using these transforms and introducing some new quantities defined below, they showed that Equations (3a, b) can be written in the following dimensionless form:

$$\left[-i\alpha + (\nu - \nu_A) \frac{dx}{dl} \frac{d}{dx} \right] \bar{f} = \bar{g}(\nu - \nu_A) \frac{dx}{dl} \frac{d\psi}{dx}, \quad (5a)$$

$$\left[-i\alpha + (\nu + \nu_A) \frac{dx}{dl} \frac{d}{dx} \right] \bar{g} = \bar{f}(\nu + \nu_A) \frac{dx}{dl} \frac{d\psi}{dx}, \quad (5b)$$

where $x = r/r_a$, and

$$dl = \frac{ds}{r_a} = \left[1 + \left(x \frac{d\theta}{dx} \right)^2 \right]^{1/2} dx, \quad (6)$$

is the arc length, and $\theta = \theta(x)$ represents the equation of the field line. In addition, the parameter α is defined by

$$\alpha = \frac{\omega r_a}{V_a} = \frac{2\pi r_a}{\tau V_a}, \quad (7)$$

with r_a describing the location of the Alfvénic critical point, ν and ν_A being the flow and Alfvén velocities normalized by the Alfvénic critical velocity V_a , and τ being the period of Alfvén waves, $\tau = 2\pi/\omega$. Because the solutions to Eqs. (5a and b) are complex, we must consider $|\bar{f}|$ and $|\bar{g}|$ to get physically meaningful quantities. It is also important to realize

that both $|\bar{f}|$ and $|\bar{g}|$ are global quantities such that they are determined at a given height by the reflection process taking place in other parts of the flow. We shall discuss this issue in more detail in the next section of this paper.

To solve Equations (5a, b), the boundary conditions have to be specified. One boundary condition is determined by a singularity in Equation (5a) which occurs at the Alfvénic critical point. To remove this singularity, H&O proposed to take $\bar{f} = 0$ at the Alfvénic critical point as the first boundary condition; this means that there is no wave reflection at the critical point and that Alfvén waves of all frequencies are moving outward in the Sun's frame of reference. Above the critical point, Alfvén waves of some frequencies may, however still be non-WKB waves. H&O also analyzed in detail the wave action for Alfvén waves and found that the Fourier amplitudes $\bar{f}(s)$ and $\bar{g}(s)$ must obey the following conservation relation

$$|\bar{g}|^2 - |\bar{f}|^2 = \text{const} . \quad (8)$$

Combining the first boundary condition with this relation, one obtains $\bar{g}(s) = \text{const}$ at the Alfvénic critical point. As a matter of convenience, one may take $\bar{g}(s) = 1$ at the Alfvénic critical point as the second boundary condition. It is interesting to note that the boundary conditions $\bar{f}(s) = 0$ and $\bar{g}(s) = 1$ are also WKB solutions to Equations (5a, b). Because the differential Equations (5a, b) and the chosen boundary conditions contain only one parameter α , the character of the solutions will be determined by this single parameter. However, it is important to realize that α depends on the wave frequency, the location of the Alfvénic critical point, and the Alfvén velocity there, which in turn are determined by the magnetic field strength and the electron density distribution. By changing these parameters we can investigate the behavior of Alfvén waves of different periods propagating in different wind models. It should be mentioned that the set of Equations (5a, b) is very stiff for large values of α . In some cases it was impossible to obtain results for periods

shorter than a few minutes, even with the use of a subroutine especially developed to treat stiff equations.

Two models of the solar wind were used by H&O, namely, the so-called Munro-Jackson model [Munro and Jackson 1977], for a polar and nonspherical coronal hole and the "spherical" model in which the parameters describing the background flow are based on an empirical density profile. To reproduce the results of H&O, we numerically integrated Equations (5a, b) subject to the boundary conditions $\bar{f} = 0$ and $\bar{g} = 1$ at the Alfvénic critical point. We have reconstructed their spherical solar wind model by using the same data adopted from Sittler [1978]. The solar wind base was set at $r_0 = 1.03R_\odot$ and physical parameters at r_0 had the following values: magnetic field $B_0 = 2 G$, electron density $n_{e_0} = 4 \times 10^8 \text{ cm}^{-3}$, temperature $T_0 = 1.3 \times 10^6 K$. Then, we calculated the Alfvén velocity with distance from the Sun and the resulting wind velocity using Eq. (1), with $r_a = 20R_\odot$, as suggested by H&O. Finally, we have reproduced quantitatively the behavior of Alfvén waves in the spherical solar wind model by changing the wave period in the range considered by H&O. We have found full agreement with their results and were able to draw the following conclusions: (i) all Alfvén waves with periods of one day and longer are non-WKB waves in the solar wind; (ii) there is an enhancement of the wave energy density for non-WKB waves when compared to that found for WKB waves; (iii) there is no corresponding enhancement of the wave energy flux density for non-WKB Alfvén waves; and (iv) non-WKB Alfvén waves are indeed no more effective in accelerating the solar wind than WKB Alfvén waves. To test the validity of these conclusions for different solar wind models, we have performed a number of parametric studies described in the following two sections.

WAVE REFLECTION

To present the results of our parametric studies, we must first describe the wind models used in our calculations. We have adapted the method developed by Yeh [1970] to construct a series of different wind models. In this method the models are calculated by specifying the

physical parameters , i.e. temperature and electron density at the sonic critical point. The mass loss rate, \dot{M} , and the polytropic index, α_p , must also be given. All models considered in this paper are calculated by taking $\dot{M} = 1.44 \times 10^{12} g s^{-1} = 2.3 \times 10^{-14} M_{\odot} yr^{-1}$ and $\alpha_p = 1.05$; these two parameters remain fixed at these values in our parametric studies. For different physical parameters at the sonic critical point, the wind models have different distributions of the wind velocity, temperature and density, and also have different values of these parameters at the base of the wind which is fixed at $r = 1.03 R_{\odot}$. This allows us to investigate Alfvén wave reflection in models that have both the distribution of basic physical parameters and their values at the base of the wind significantly different than used by H&O. The decision to perform parametric studies in different wind models is justified because there are no commonly accepted coronal and wind models based on observational data.

The method applied in this paper to construct the coronal and wind models allows us to perform three types of parametric studies. First, we may investigate Alfvén wave reflection in models characterized by the same density and temperature at the base of the wind but having a different value of the magnetic field strength there. Second, we may study the dependence of wave reflection on changes in the density at the base by assuming that both the base magnetic field and the base temperature are fixed; it must be noted that the method chosen here to construct the wind models does not formally allow us to fix the temperature at the base and at the same time to vary the base density [Yeh 1970]. Therefore our study is restricted to a narrow range of temperatures that changes the base density by approximately a factor of 2. Finally, we fixed the magnetic field strength at the base and calculated wind models for four different values of the base temperature; as mentioned above, this automatically leads to four different values of the density at the base. For each of these cases, we solve the wave equations (5a, b) to find the functions $|\bar{f}|^2$ and $|\bar{g}|^2$. In addition, to compare our results with those previously obtained, we calculate the reflection coefficient. As discussed by Leroy [1980], some caution is required

in properly defining the reflection coefficient. Namely, one must clearly identify a region in the wind model where wave reflection does not occur, so that Alfvén waves existing in this region are outward propagating (WKB) waves in the Sun's frame of reference. Assuming that the region exists in the wind model, then the transmission coefficient is defined as the ratio of the wave energy carried by the outward propagating waves at the base to that carried by these waves in the region without reflection. In the approach considered in this paper, Alfvén waves of all frequencies have $\bar{f} = 0$ at the Alfvénic critical point; beyond that point the solar wind convects inward waves outward in the Sun's frame of reference. There may still be reflection beyond the critical point, so that some waves move inward in the solar wind frame, but this does not affect the reflection coefficient. Our calculations demonstrate that in most of our models waves with periods of the order of one day and shorter are also WKB waves beyond the critical point. Therefore, we use the location of the Alfvénic critical point to identify the region beyond which all waves propagate outward for our definition of the reflection coefficient. To derive the expression for the reflection coefficient, we begin with the conservation of wave action, N , written in the following form:

$$\frac{\partial N}{\partial t} + \nabla \cdot (\mathbf{V}_g N) = 0, \quad (9)$$

where

$$N = \rho V \left(\frac{g^2}{V + V_A} - \frac{f^2}{V - V_A} \right), \quad (10)$$

and \mathbf{V}_g is the group velocity of Alfvén waves. After taking the time average of Eq. (9), we find that $\nabla \cdot (\mathbf{V}_g \bar{N}) = 0$ because the time average of the first term vanishes; this can be also written as $r^2 V_g \bar{N} = \text{const}$, where \bar{N} is the averaged wave action. Now, we may define the reflection coefficient, \mathcal{R} , for the outward propagating Alfvén waves as $\mathcal{R} = 1 - \mathcal{T}$, where the transmission coefficient, \mathcal{T} , is given by

$$\mathcal{T} = \frac{(r^2 V_g \bar{N}_{out})_c}{(r^2 V_g \bar{N}_{out})_o}, \quad (11)$$

with the subscript “c” and “o” denoting the values of the considered quantities at the Alfvénic critical point and at the wind base, respectively. Substituting Eq. (10) for the outward propagating waves only into Eq. (11) and using $V_g = V + V_A$, we find that $\mathcal{T} = 1/|\bar{g}_o|^2$ and that $\mathcal{R} = |\bar{f}_o|^2/|\bar{g}_o|^2$. The reflection coefficient allows estimating the total amount of wave energy reflected between the base of the wind model and the location of the Alfvénic critical point.

Before we present the results of our studies, we first want to briefly discuss a simple physical picture of wave reflection which emerges from geometrical optics and can be helpful in understanding the wave behavior in different wind models. In this picture, a nominal wavelength λ for an Alfvén wave of a given period τ is defined at each height in the wind model as $\lambda = V_A \tau$. Because the background medium is inhomogeneous, both V_A and λ must be functions of height. Now, as known from geometrical optics the wave propagation is affected by the inhomogeneity of the medium only when the wavelength becomes comparable or longer than the characteristic wave velocity scale height. Applying this to our case, we have $\lambda \approx H_A = V_A/(|dV_A/dx|)$, where H_A is the Alfvén velocity scale height; note that H_A accounts directly for the density and magnetic field gradients and that both the temperature and wind velocity gradients have only indirect effects. It can be shown that for any wave-bearing medium, reflection is weak when $\lambda \ll H_A$ and that it becomes strong when $\lambda \gtrsim H_A$. Obviously, the above criteria are too simple to quantify the process of Alfvén wave reflection in a wind model in any detail but they are helpful in understanding the results based on the solutions of the Alfvén wave equations (5a and b) and interpreting the behavior of the wave amplitudes $|\bar{f}|^2$ and $|\bar{g}|^2$.

The results of our parametric studies are presented in six-panel figures (see Figures 1, 2 and 3). The first three panels in each figure show distributions of density, temperature, and Alfvén and wind velocity with distance from the Sun. In the next two panels, we present changes in the wave (Fourier) amplitude $|\bar{f}|^2$ caused by different wind models and wave periods; note that once $|\bar{f}|^2$ is known, $|\bar{g}|^2$ can always be calculated by using Eq.

(8) with $const = 1.0$. Finally, the last panel shows the reflection coefficient as a function of wave period. In the following, we discuss in detail the results presented in Figures 1, 2 and 3.

In our first parametric study we calculated the temperature and density distributions according to the method described above, getting the temperature and the electron density at the base to be $T_0 = 1.6 \times 10^6$ K and $n_{e0} = 7.0 \times 10^7$ cm^{-3} , respectively. This we call Model 1 (see Figs. 1a and b). Because the strength of magnetic fields in solar coronal holes is presently not well known [e.g., Parker, 1991], we have assumed that the field can range from 2 G to 15 G, and preferentially is of the order of 10 G [e.g., Moore et al. 1991]. Any changes in the strength of the magnetic field at the solar wind base give different Alfvén velocities which lead to different locations of the Alfvénic critical point (see Fig. 1c) and give different models. If the wave frequency ω is held constant for all models with different magnetic field strengths, then the parameter α is different for each location of the Alfvénic critical point and we expect different wave behavior in each model. The waves propagating in the model with the strongest magnetic field will have the longest wavelengths and, according to the above criteria, will be reflected more than waves of the same frequency propagating in other models with weaker magnetic fields. In addition, it must be noted that reflection decreases with distance from the model base and becomes zero at the point where the Alfvén velocity has a maximum; as this point is approached, $H_A \rightarrow \infty$, and the medium can be treated locally as homogeneous. Bearing this result in mind, we now show the dependence of the wave amplitude $|\tilde{f}|^2$ solely on the magnetic field strength. We fixed the wave period to be $0.04^d \approx 1^h$ and plotted $|\tilde{f}|^2$ versus the distance from the base (see Fig. 1d). The figure clearly shows that the value of $|\tilde{f}|^2$ increases with increasing magnetic field strength and that it is greatest at the base of each wind model. As seen in Figure 1e, the wave amplitude $|\tilde{f}|^2$ goes through a local maximum where the Alfvén velocity peaks (this occurs at the point where $d\psi/dz = 0$, see also Eqs. 5a and b) and that it is practically zero above $10R_\odot$. To understand the results presented in

Figure 1d, we must now recall our interpretation of the function $|\tilde{f}|^2$ given in the previous section. As discussed before, the wave amplitude $|\tilde{f}|^2$ is not a local quantity but instead it is determined by the reflection process taking place everywhere in the model; more specifically, because of the boundary condition imposed on \tilde{f} at the Alfvénic critical point, each model can be formally divided into the lower (from the base to the critical point) and upper (from the critical point to infinity) part, and the local value of $|\tilde{f}|^2$ is determined by the global wave behavior in each part separately. In other words, the wave amplitude $|\tilde{f}|^2$ reveals how important non-WKB effects are globally in the model ($|\tilde{f}| = 0$ for WKB waves) and its value at any height provides information about the global reflection process occurring above this height; the local value of $|\tilde{f}|^2$ does not indicate, however, whether reflection is locally strong or weak (see below for more details). Therefore, the fact that $|\tilde{f}|^2$ has a maximum at the same location as the maximum of the Alfvén velocity does not mean that the maximum of reflection occurs there. It rather indicates that there is a region of strong reflection below and above the location of the maximum of the Alfvén velocity, and that this leads to the formation of the region where waves can be trapped thereby causing the calculated enhancement of $|\tilde{f}|^2$. To identify the height in the model where the strongest wave reflection occurs, one must calculate the derivative of $|\tilde{f}|^2$ with respect to x , take its absolute value, and then plot it versus distance. The maxima and zeros of the absolute value of $d|\tilde{f}|^2/dx$ are located at these heights where wave reflection is locally the strongest and weakest, respectively. For example, by taking the real and imaginary part of the function $|\tilde{f}|^2$ and using Eqs. (5a and b), one may find that $d|\tilde{f}|^2/dx = 0$ at the point where $d\psi/dx = 0$ (the maximum of the Alfvén velocity). This is consistent with the physical picture discussed above which requires no reflection at the point where $dV_A/dx = 0$. Even though, we do not show the plots of the derivative with distance, the results presented in Figure 1d clearly indicate that the region of strongest wave reflection is located at the base in all considered models. As expected, the weakest wave reflection ($d|\tilde{f}|^2/dx = 0$) always occurs at the maximum of the Alfvén velocity.

We now investigate the dependence of the wave amplitude $|\bar{f}|^2$ on the wave period (see Fig. 1e). The presented results demonstrate that $|\bar{f}|^2$ increases with increasing wave periods and for sufficiently long periods reaches a maximum at the peak of the Alfvén velocity. In the light of our discussion of $|\bar{f}|^2$, this coincidence simply indicates that locally wave reflection decreases toward the peak and that it reaches zero at the location of the maximum of the Alfvén velocity. Recalling now our interpretation of the wave amplitude $|\bar{f}|^2$, it is seen from Figure 1e that long period Alfvén (say, 5 days) waves are more strongly reflected in the model than those with shorter periods. Note that waves with periods of 5 days and longer are non-WKB waves even beyond the critical point and that this agrees with the discussion in H&O of the behavior of these waves when the parameter α reaches a certain value, approximately 0.5 and less. Finally, results presented in Figure 1f show that the reflection coefficient \mathcal{R} , defined according to our Eq. (11), also increases with increasing magnetic field strengths and wave periods. Even Alfvén waves with periods of the order of several days are only marginally reflected in our wind model providing that the magnetic field is not very strong, ($B_o = 2G$). For stronger fields there is always a range of wave periods for which the reflection coefficient remains constant. This seems to be in contradiction with the results presented in Figures 1d and 1e, which instead demonstrate that non-WKB effects should be more prominent when the magnetic field strength and/or the wave period are increased. The discrepancy is discussed in more detail in the next paragraph of this section.

The results presented in Figure 2 show the dependence of Alfvén wave reflection on two wind models (Models 2 and 3, see Figs. 2a and b) which have similar distributions of temperature and density but two different values of these parameters at the base: $T_o = 1.28 \times 10^6$ and 1.35×10^6 K; these two temperatures correspond to the following values of the base density: $n_{eo} = 7.0 \times 10^8$ and 3.75×10^8 cm^{-3} . Note that the distribution of temperature and density in both models is very similar and that the main difference between the models is the different value of the density at the base; the latter obviously

affects the value of the Alfvén velocity at the base and leads to slightly larger Alfvén velocity scale height, H_A , in Model 3. This explains the results presented in Figure 2d, which show that waves of the same period are more non-WKB waves in Model 2 than in Model 3 because the condition $\lambda \gtrsim H_A$ is first satisfied in Model 2 as the frequency is decreased. It must be also noted that the derivative $d|\bar{f}|^2/dx$ is greatest in both models at the base which, according to our earlier discussion, indicates that locally the strongest wave reflection occurs there. The results presented in Figure 2e demonstrate similar wave behavior as that shown in Figure 1e. There is, however, a new interesting feature that can be seen for waves of period equal to 1 day. The dip observed at $x \approx 1.2$ is related to the fact that there is a change in the local density (as well as in Alfvén velocity) scale height and that this change affects locally wave reflection; therefore, the derivative $d|\bar{f}|^2/dx$ goes through another zero (no reflection at this point). Figure 2f shows more convincingly than Figure 1f that after constant increase of the \mathcal{R} value with the period, there are frequencies for which reflection has a minimum and then starts to increase again.

The described type of behavior is called “a tunneling effect” [e.g., Velli et al. 1993; Lou and Rosner 1993] to emphasize the fact that a travelling wave of a certain frequency can appear beyond the region of strong reflection as a propagating wave with some portion of its energy being lost due to reflection. To understand the origin of this effect, we now compare the results presented in Figures 2e and 2f. It is seen that only the plot of the reflection coefficient clearly indicates the existence of the tunneling effect. The plot of the function $|\bar{f}|^2$ shows instead that non-WKB effects (stronger reflection) become more prominent for longer wave periods. Note that a similar discrepancy is briefly mentioned in the previous paragraph. The discrepancy between the results obtained by using $|\bar{f}|^2$ and \mathcal{R} is primary caused by the fact that the latter is defined in terms of $|\bar{f}|^2$ and $|\bar{g}|^2$ at the model base, and that values of these functions at the base are determined by the global wave behavior in the lower part of the model. The fact that this global behavior may be complicated is clearly shown in Figure 2e (see also Fig. 1e). Again, it is helpful to consider

the derivative of $|\bar{f}|^2$ with respect to x , take its absolute value, and find the location of maxima and zeros. It is found that $d|\bar{f}|^2/dx$ for waves with periods of the order of 0.1 day and shorter has only one maximum at the base. However, for waves with periods of the order of 1 day, there are clearly two maxima corresponding to regions of locally strong wave reflection; note that these regions are located symmetrically on both sides of the point where no reflection occurs ($dV_A/dx = 0$). If waves of certain periods are trapped between these two regions, then, changes in the global distribution of $|\bar{f}|^2$ (i.e, formation of a local maximum) are expected. As a result of those changes, the values of $|\bar{f}|^2$ and $|\bar{g}|^2$ at the base become lower for long period waves than for short period waves (see Fig. 2e). This causes the wave reflection as measured by the value of the reflection coefficient to be stronger for short period waves. It is evident from the above discussion that this variation of the reflection coefficient with period is potentially misleading because in reality long period waves are more non-WKB waves than short period waves. This also means that the result may lead to a misinterpretation of Alfvén wave reflection, in particular, if the reflection coefficient is solely used to study the wave behavior.

After studying the influence of the magnetic field and density on the reflection of Alfvén waves, we now proceed to the overall model dependence. We constructed four distinct wind models characterized by the same magnetic field at the base ($B_0 = 10G$) but with the base temperature ranging from $7.45 \times 10^5 K$ to $1.51 \times 10^6 K$ (Models 4 - 7, see Fig. 3a); this corresponds to the base density ranging from $5.0 \times 10^{13} cm^{-3}$ to $6.55 \times 10^7 cm^{-3}$ (see Fig. 3b). Although the high density at the base in Model 4 seems to be unrealistic for the Sun, we include this model into our parametric studies to see the effect caused by this extreme case on Alfvén wave reflection (see Fig. 3b, for comparison to Sittler's model). As shown in Figures 3d and 3f, the efficiency of Alfvén wave reflection in this particular model is very low but increases in wind models with higher temperature and lower density. Figure 3e presents similar behavior of the wave amplitude $|\bar{f}|^2$ as that observed in Figure 2e. Waves with periods 0.04^d have their local maximum where waves with periods 5^d have

their local minimum. This is strong evidence for a complicated behavior of Alfvén waves in both discussed models. In the light of our discussion of the results presented in Figures 1 and 2, it is now easy to understand the behavior of Alfvén waves of different periods in different solar wind models. The main conclusion is that Alfvén waves are more efficiently reflected in models with the base temperature higher than 10^6 K and with the base density lower than $7 \times 10^7 \text{ cm}^{-3}$. The results presented in Figure 3f also indicate that Alfvén waves must have periods of at least several hours in cooler and denser atmospheres in order to be strongly reflected ($\mathcal{R} \geq 50\%$). This is in contrast with the results obtained by H&O who showed that only waves with periods of one day or longer are strongly reflected in the solar wind. The difference can be easily explained by the fact that the efficiency of Alfvén wave reflection is strongly model dependent. As we said earlier, using the global reflection coefficient to infer how freely waves propagate can be misleading. This is due to the fact (as explained in the previous paragraph) that the value of $|\bar{f}|^2$ at the base may become smaller even when periods increase. This again implies that the results based solely on the global reflection coefficient must be taken with caution.

In all calculations described here, the condition $|\bar{g}|^2 - |\bar{f}|^2 = \text{const}$ has been checked for each radial distance. We have found that the condition has always been satisfied with accuracy better than 1% in the inner (below the Alfvénic critical point) part of the solar wind model and that the accuracy is slightly lower far beyond the Alfvénic critical point. The discrepancy is due to the nature of Eqs. (5a, b), which are stiff for large values of α . However, this numerical check on our accuracy gives us full confidence in our results.

WAVE ACCELERATION

One of the main conclusions from the H&O paper is that non-WKB Alfvén waves are no more effective in accelerating the solar wind than WKB waves. As discussed earlier in this paper, some recent results seem to lead to the opposite conclusion [Barkhudarov 1991, Velli 1993]. Here, we verify the H&O results by calculating the wave acceleration

for WKB and non-WKB Alfvén waves. Following the formalism of H&O in deriving the formula for the wave acceleration, the proper way to calculate the acceleration force, which is caused by the propagating waves and acts on the background medium, is to consider the conservation of wave energy [e.g., Dewar 1970, Jacques 1977, H&O]. The wave energy conservation equation is

$$\frac{\partial \epsilon}{\partial t} + \nabla \cdot \mathbf{E} = -\mathbf{f}_w \cdot \mathbf{V}, \quad (12)$$

with the wave energy density, ϵ , being defined by

$$\epsilon = \frac{1}{2} \rho (V_\phi^2 + V_{A\phi}^2), \quad (13)$$

the wave energy flux, \mathbf{E} , being given by

$$\mathbf{E} = \rho \mathbf{V} \left(\frac{1}{2} V_\phi^2 + V_{A\phi}^2 - \eta^{1/2} V_\phi V_{A\phi} \right), \quad (14)$$

and with the work done by the waves on the background medium being described by

$$\mathbf{f}_w \cdot \mathbf{V} = \frac{\rho V_R}{R} (V_\phi^2 - V_{A\phi}^2) - \mathbf{V} \cdot \nabla \frac{B_\phi^2}{8\pi}. \quad (15)$$

After taking the time average of Eq. (12) and using Eq. (14), we obtain

$$\mathbf{f}_w \cdot \mathbf{V} = -\frac{1}{2} \rho \mathbf{V} \cdot \nabla \left[\frac{1}{2} |\tilde{V}_\phi|^2 + |\tilde{V}_{A\phi}|^2 - \eta^{1/2} \text{Re}(\tilde{V}_\phi^* \tilde{V}_{A\phi}) \right], \quad (16)$$

which gives the expression for the wave acceleration

$$\mathbf{a} = -\frac{d}{ds} \left(\frac{\bar{E}}{\rho V} \right), \quad (17)$$

where the averaged wave energy flux, \bar{E} , is defined by

$$\bar{E} = \frac{1}{2} \rho V \left[\frac{1}{2} |\tilde{V}_\phi|^2 + |\tilde{V}_{A\phi}|^2 - \eta^{1/2} \text{Re}(\tilde{V}_\phi^* \tilde{V}_{A\phi}) \right]. \quad (18)$$

Note that our formula for the wave acceleration (Eq. 17) differs from that used by H&O by a factor of 1/2 (see their Eq. 95). In our studies, Eq. (17) has been used to calculate

the wave acceleration in the wind models described in the previous section. The results are presented in Figure 4. We shall now discuss these results in detail.

Our intention here is to investigate the dependence of wave acceleration on the magnetic field strength at the base (Fig. 4a) and the wave period (Fig. 4b). The results presented in these figures clearly indicate that the wave acceleration decreases (i) when the magnetic field strength at the base increases and (ii) when Alfvén waves with periods of several hours or longer are considered. As shown in the previous section, however, these are the cases when wave reflection increases and non-WKB effects become important. Therefore, we may conclude that the wave acceleration decreases for non-WKB waves. This rather surprising result can be explained by the following simple example. Let us consider a short period (say, several minutes) and a long period (say, several hours) Alfvén wave entering the wind model at the base and carrying the same amount of energy; in the approach used here the waves of different frequencies carry approximately the same energy. In all our wind models, the short period wave will propagate without any reflection but will exert the acceleration force on the background medium; the force is a local quantity and is proportional to the gradient of wave energy flux divided by the mass flux (see Eq. 17). The long period wave will undergo strong reflection and at a given height will always have much less energy available for exerting the acceleration force than the short period wave. This means that among WKB and non-WKB waves which carry comparable amount of energy, the former are always more effective in exerting a force on the background medium. The situation may be completely different, however, if the long period wave has a larger amplitude than the short period wave and thereby carries much more energy; the complete discussion of this problem is beyond the scope of this paper because it would involve a nonlinear wave treatment.

The results presented and discussed above show why WKB waves are more effective in accelerating the background medium than non-WKB waves; it must be noted, however, that this result is valid only in a linear regime and when waves are initially assumed to

carry the same amount of energy. The problem we discuss now is the dependence of wave acceleration on different wind models. The results of our calculations are shown in Figures 4c and 4d. In Fig. 4c, we plot the wave acceleration for the four different models described in the previous section. The main differences between the models are the values of physical parameters at the base (for example, in Model 4 the base temperature is the lowest and the base density is the highest; however, in Model 7 the base temperature is the highest and the base density is the lowest). In all models, we take the same magnetic field strength ($B_o = 2 G$) and the same wave period (0.04^d); it can be shown that Alfvén waves with this period are WKB waves in all our models, since their function $|\bar{f}|^2$ is either zero or stays close to zero everywhere in the model. Now, the results shown in Fig. 4c indicate that the wave acceleration is strongly model dependent (one could expect similar wave acceleration for the same WKB waves) and that it is the strongest for Model 7 and the lowest for Model 4. Because the results presented in Fig. 3f demonstrate that the efficiency of wave reflection increases from Model 7 to Model 4, with the exception of Model 6, one could therefore conclude that there is a contradiction between the results presented in Fig. 4c (stronger reflection leads to stronger acceleration) and those shown in Fig. 4a and 4b (stronger reflection gives lower acceleration). To show that this conclusion is not correct, we perform the following calculations. We set the magnetic field strength and the wave period in such that the considered Alfvén waves are primarily non-WKB waves in Model 7 and almost WKB waves in Model 4; it must be remembered that by taking stronger magnetic fields we are allowing for more non-WKB effects. The results of our calculations are presented in Fig. 4d. First, we compare the wave acceleration in Model 4 and 7 obtained for $B_o = 2 G$, and find a similar trend as that shown in Fig. 2c for Models 2 and 3. Then, we compare the wave acceleration in Model 4 and 7 but for $B_o = 10 G$ to see that it has been reduced significantly by non-WKB effects and only slightly exceeds that obtained for waves in Model 4 that are nearly WKB waves. Finally, we compare the wave acceleration calculated in Model 4 for $B_o = 2 G$ (almost WKB waves) with that

obtained in Model 7 for $B_0 = 10$ G (strongly non-WKB waves). The comparison in Fig. 4d shows that non-WKB effects reduce the wave acceleration and that it becomes even less effective than in Model 4; note that according to Fig. 4c, Model 4 has the lowest wave acceleration. In summary, the wave acceleration is strongly model dependent and it decreases with increasing non-WKB effects.

The problem we want to address now is whether WKB waves are more effective in accelerating the solar wind than non-WKB waves. Despite the results we have obtained the problem is not trivial, because there is one additional condition that must be obeyed. The condition requires that the maximum of the wave acceleration occurs in the solar wind above the sonic critical point. As shown by Leer and Holzer (1980), only in this case can the deposited wave momentum be used to drive the solar wind to the observed large asymptotic flow speed. We have also studied this problem and the results are presented in Fig. 5, where we plot the location of the maximum of wave acceleration with respect to the location of the sonic critical point for two different wind models. The figure shows that longer period Alfvén waves (primarily non-WKB waves) have maximum wave acceleration located farther above the sonic critical point than shorter period waves (primarily WKB waves). It is also seen that the range of wave periods which leads to this is extremely sensitively to the wind model. Our order of magnitude estimates (we use the H&O method of converting dimensionless variables into their physical values) indicate that in most cases even WKB waves exert a force which is too small to accelerate the wind; the obtained result is, however, affected by the constraint that the considered Alfvén waves carry roughly the same amount of energy despite their periods. In addition, as we clearly presented in Figs. 3 and 4, all the results are strongly model dependent and it can be shown that for some cases the wave acceleration can exceed the wind acceleration before the sonic critical point. Therefore, one can expect that Alfvén waves could play an important role in the atmospheres of other stars.

CONCLUDING REMARKS

In this paper, we discussed the behavior of non-coupled, undamped, linear and toroidal Alfvén waves. Our studies indicate that both wave reflection and wave acceleration are strongly model dependent so that it is difficult to predict the atmospheric response to the waves without an appropriate wind model. The range of models considered in this paper allows us to draw several important conclusions. They can be summarized as follows:

- (1) Alfvén waves undergo substantial reflection, providing that base magnetic field strength B_0 is at least $10G$ and/or the wave period is in the range of hours or longer.
- (2) The strongest reflection can be expected in solar wind models with the base temperatures higher than 10^6 K and with the base densities lower than $7 \times 10^7 \text{ cm}^{-3}$ (neither of these values contradict presently known observational data). In these models as well as in the models with lower temperatures and higher densities, Alfvén waves with periods as short as several minutes can be treated as WKB waves; for Alfvén waves with periods of the order of one hour or longer a non-WKB treatment is required.
- (3) The region of strongest wave reflection is usually located at the base of the models.
- (4) The variation of the reflection coefficient with period can be misleading because it often shows that short period waves are more reflected than long period waves; in reality the latter are always more non-WKB waves than the former.
- (5) Finally, non-WKB, linear Alfvén waves are always less effective in accelerating the plasma than WKB Alfvén waves.

In addition to these conclusions, we have attempted to give the physical reasons for our result. In the following, we shall compare the presented results to those previously obtained.

We begin with the comparison to the H&O results. The main difference is that our studies demonstrate that both Alfvén wave reflection and Alfvén wave acceleration are strongly model dependent. In addition, we show that in some wind models Alfvén waves with periods as short as one hour must be treated as non-WKB waves. Our results

concerning the wave acceleration are in agreement with those obtained by H&O but they are in contradiction with some results obtained by Barkhudarov [1991] and Velli [1993] who found that non-WKB Alfvén waves of certain frequencies can be more effective in accelerating the plasma than WKB waves; this is exactly opposite to one of the main conclusions of this paper. Velli [1993] also calculated the dependence of the transmission coefficient of Alfvén waves on their periods and found that it is very sensitive to the temperature both in a static atmosphere and in an isothermal solar wind. In the case of a static atmosphere, only waves with periods less than about 15 minutes are completely transmitted whereas in the case of the moving atmosphere, he showed that the transmission coefficient generally increased even for periods in the range of tens of days. He claimed that this type of behavior is due to the changes in the temperature in his isothermal models. We also differ from Velli in that we show significant reflection for long period waves; his transmission coefficient almost equals unity for these periods. This is likely explained by using his Eq. (25) and the adjustment of the value of the Alfvén velocity at the solar surface and at the Alfvénic critical point to nearly the same value, which is not the case in our studies. This tuning of Alfvén velocities might be an artificial effect of computing his Alfvén velocity profile and may also affect his calculations of the wave acceleration. In general, Velli and his co-workers have drawn a number of conclusions concerning Alfvén wave reflection by using the transmission (reflection) coefficient. As shown in this paper, interpretation of results based solely on the concept of the reflection coefficient can be misleading because it often reveals that short period waves are more reflected than long period waves; in reality the opposite is true.

Finally, our results related to the effectiveness of reflection for short period waves seems to be in contradiction with the previous claims made by Moore et al. [1991]. They found that for a static, isothermal and radially spreading coronal hole with $B_o = 10 G$ at $r_o = 1.15R_\odot$ all waves with periods longer than several minutes should be reflected if the temperature at the base is less than $1.0 \times 10^6 K$, and should escape to the solar wind

if that temperature is higher than $1.0 \times 10^6 K$. They suggested that these short period (reflected) Alfvén waves are responsible for the heating in solar coronal holes. The results obtained in this paper for non-isothermal models clearly indicate that Alfvén waves with periods as short as several minutes cannot be reflected in the solar wind models; similar results have been obtained when we considered isothermal models. Therefore, we conclude that the approach presented by these authors must be revised.

ACKNOWLEDGMENT

Part of this work was done while MK visited the Center for Space Plasma and Aerodynamic Research at the University of Alabama in Huntsville, and ZEM visited the Institute for Theoretical Physics and Astrophysics at the University of Gdansk in Poland. During those visits MK and ZEM were supported by NSF under grant INT-9016514 and by the Polish Committee for Scientific Research of the Polish Academy of Sciences under grant PB 22106-91-02. In addition, ZEM acknowledges partial support of this research by NASA under grants NAGW-2933 and NAG8-839, and by NSF under grant ATM-9119580. The research was completed while SFN held an NRC Research Associateship at NASA/MSFC.

REFERENCES

- An, C. H., Musielak, Z. E., Moore, R. L., and S. T. Suess, Reflection and trapping of transient Alfvén waves propagating in an isothermal atmosphere with constant gravity and uniform magnetic field, *Astrophys. J.*, *345*, 597, 1989.
- An, C. H., Suess, S. T., Moore, R. L., and Z. E. Musielak, Reflection and trapping of Alfvén waves in a spherically symmetric stellar atmosphere, *Astrophys. J.*, *350*, 309, 1990.
- Barkhudarov, M. R., Alfvén waves in stellar winds, *Solar. Phys.*, *135*, 131, 1991.
- Barnes, A., Acceleration of the solar wind, *Rev. Geophys.*, *30*, 43, 1992.
- Belcher, J., Alfvénic wave pressures and the solar wind, *Astrophys. J.*, *168*, 509, 1971.
- Belcher, J., and L. Davis, Large-amplitude Alfvén waves in the interplanetary medium, *J. Geophys. Res.*, *79*, 3534, 1971.
- Belcher, J., and S. Olbert, Stellar wind driven by Alfvén waves, *Astrophys. J.*, *200*, 369, 1975.
- Campos, L. M. B. C., On waves in gases. Part II: Interaction of sound with magnetic and internal modes, *Rev. Mod. Phys.*, *59*, 363, 1987.
- Dewar, R. L., Interaction between hydromagnetic waves and a time dependent, inhomogeneous medium, *Phys. Fluids*, *13*, 2710, 1970.
- Ferraro, V. C. A., On the reflection and refraction of Alfvén waves, *Astrophys. J.*, *119*, 393, 1954.
- Ferraro, V. C. A., and C. Plumpton, Hydromagnetic waves in a horizontally stratified atmosphere, *Astrophys. J.*, *127*, 459, 1958.
- Heinemann, M., and S. Olbert, Non-WKB Alfvén waves in the solar wind, *J. Geophys. Res.*, *85A*, 1311, 1980.
- Hollweg, J. V., Alfvén waves in the solar wind: Wave pressure, Poynting flux, and angular momentum, *J. Geophys. Res.*, *78*, 3643, 1973.

- Hollweg, J. V., On WKB expansions for Alfvén waves in the solar wind, *J. Geophys. Res.*, **95**, 14873, 1990.
- Jacques, S. A., Momentum and energy transport by waves in the solar atmosphere and solar wind, *Astrophys. J.*, **215**, 942, 1977.
- Jacques, S. A., Solar wind models with Alfvén waves, *Astrophys. J.*, **226**, 632, 1978.
- Leer, E., and T. E. Holzer, Energy addition in the solar wind, *J. Geophys. Res.*, **85**, 4681, 1980.
- Leroy, B., Propagation of waves in an atmosphere in the presence of a magnetic field. II. The reflection of Alfvén waves, *Astron. Astrophys.*, **91**, 136, 1980.
- Lou, Y-Q., and R. Rosner, Reflection of Alfvén waves in stellar atmospheres: The case of open magnetic fields, *submitted to Astrophys. J.*, 1993.
- Moore, R. L., Musielak, Z. E., Suess, S. T. and C. H. An, Alfvén wave trapping, network microflaring, and heating in solar coronal holes, *Astrophys. J.*, **378**, 347, 1991.
- Munro, R. H., and B. V. Jackson, Physical properties of the polar coronal hole from 2 to 5 R_{\odot} , *Astrophys. J.*, **213**, 874, 1977.
- Musielak, Z. E., Fontenla, J. M., and R. L. Moore, Klein-Gordon equation and reflection of Alfvén waves in nonuniform media, *Phys. Fluids*, **4**, 13, 1992.
- Parker, E. N., Heating solar coronal holes, *Astrophys. J.*, **372**, 719, 1991.
- Rosner, R., Low, B. C., and T. E. Holzer, Physical processes in the solar corona, *Physics of the Sun*, ed. P. A. Sturrock, (New York: Reidel), Ch. 11 (Vol. II, pp.135-180), 1986.
- Sittler, E. C. Jr., Study of the electron component of the solar wind and magnetospheric plasma, Ph.D. thesis, Mass. Inst. of Technol., Cambridge, Mass., 1978.
- Thomas, J. H., Magneto-atmospheric waves, *Ann. Rev. Fluid Mech.*, **15**, 321, 1983.
- Velli, M., On the propagation of ideal, linear Alfvén waves in radially stratified stellar atmospheres and winds, *Astron. Astrophys.*, **270**, 304, 1993.

- Velli, M., Grappin, R., and A. Mangeney, Waves from the Sun?, *Geophys. Astrophys. Fluid Dynamics*, **62**, 101, 1991.
- Yeh, T., An explicit solution for polytrope solar wind equations, *J. Geophys. Res.*, **75**, 6309, 1970.

FIGURE CAPTIONS

Fig. 1. Reflection of Alfvén waves in the solar wind Model 1 (polytropic index $\alpha_p = 1.05$ here and in all succeeding models). a) Temperature distribution with $T_o = 1.63 \times 10^6 K$. b) Electron density ($n_{e0} = 8 \times 10^7 cm^{-1}$) compared with that used by Heinemann & Olbert, called "Sittler's model". c) Different values of the magnetic field at the base of corona, 2, 5, 10 and 15 Gauss, respectively, result in different profiles of Alfvén velocity. Solid line denotes a wind velocity consistent with the calculated atmosphere model. d) Radial dependence of the wave amplitude $|f|^2$ for magnetic fields corresponding to these in panel (c). e) A case study of $|f|^2$ versus distance for waves of different period with a constant value of $B_o = 10G$ at the base of the model. f) The reflection coefficient, \mathcal{R} , as a function of wave period for four different magnetic field strengths, B_o .

Fig. 2. Reflection of Alfvén waves in the solar wind Models 2 and 3, with differing base density but nearly the same temperature. a) The temperature profiles $T_o = 1.28 \times 10^6$ and $T_o = 1.35 \times 10^6$ for Model 2 and Model 3, respectively. b) The density profiles. Initial electron densities are 7.0×10^8 and $3.75 \times 10^8 cm^{-3}$, respectively. c) The wind and Alfvén velocities for both models. d) The wave amplitude $|f|^2$ in these models for field $B_o = 10 G$ and period $\tau = 0.04^d$. e) Wave reflection versus distance for Model 2 for different wave periods. f) The reflection coefficient, \mathcal{R} , is plotted as a function of wave period for both considered models.

Fig. 3. Alfvén wind reflection in wind models with strongly differing base density and temperature. a) Temperature distributions for the four models with the extreme ones differing by a factor of two (Model 4 and Model 7, respectively). b) Density profiles. The

difference between respective electron densities spans 5 orders of magnitude, with higher temperature corresponding to the lower density. c) Alfvén speeds and flow speeds. Despite the huge differences between densities, Alfvénic critical point locations and corresponding critical velocities, are concentrated around similar values. The magnetic field is 10 Gauss for all cases. d) The wave amplitude $|f|^2$ for the four models. e) Dependence of $|f|^2$ on the wave period in Model 5 with a fixed magnetic field of 10 Gauss at the base of the atmosphere. The maximum for wave with $\tau = 0.04^d$ and local minimum for wave with $\tau = 5^d$ are located at the point where density distribution changes its dependence with the distance. f) The reflection coefficient, \mathcal{R} , as a function of period for the four models.

Fig. 4. The dimensionless wave acceleration as a function of radial distance from the Sun for several models. a) Effect of varying field strength in Model 7 (see Fig. 3). b) Effect of varying wave period in Model 7. c) Models 4 - 7 compared. d) Models 4 and 7 for the field strengths 2 Gauss and 10 Gauss.

Fig. 5. The difference between the location of the point where acceleration has its maximum and the location of the sonic point (where the wind velocity equals to the local sound speed) as a function of wave period. This difference is plotted for Models 5 and 7 (see Fig. 3).

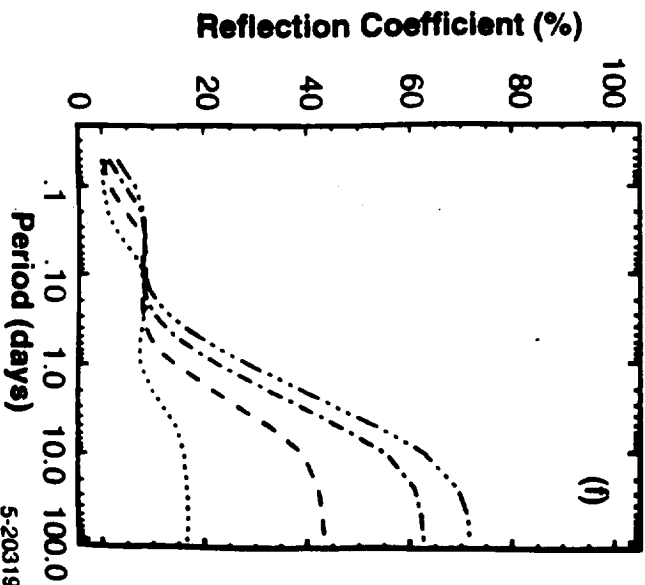
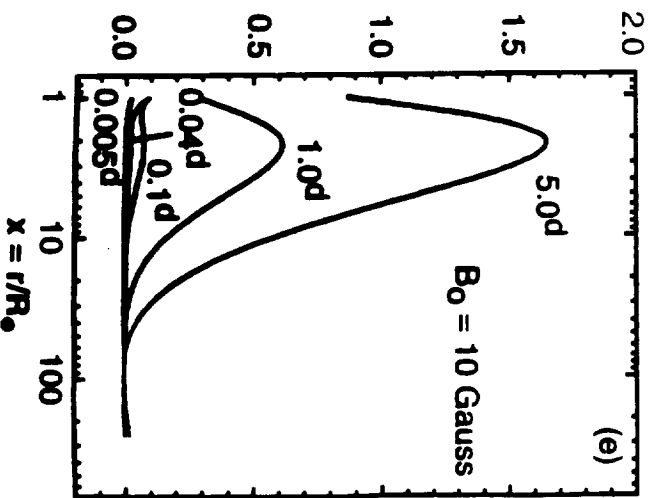
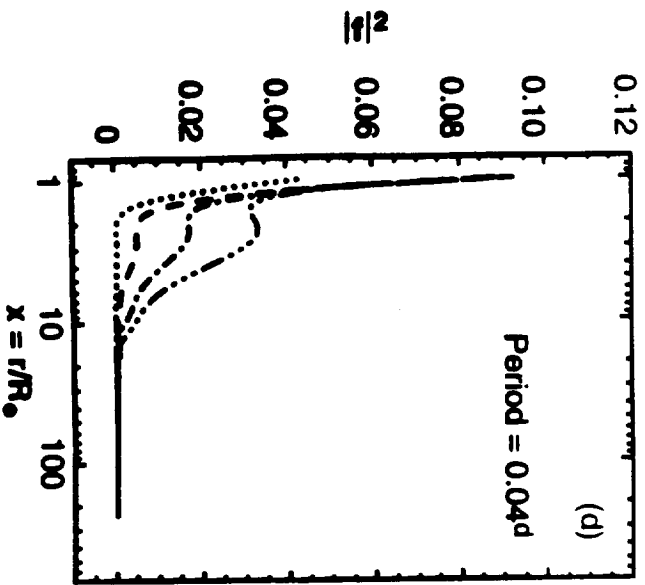
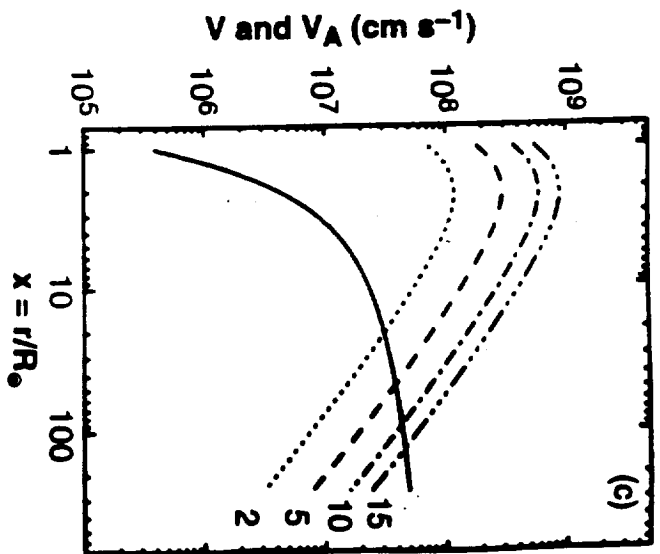
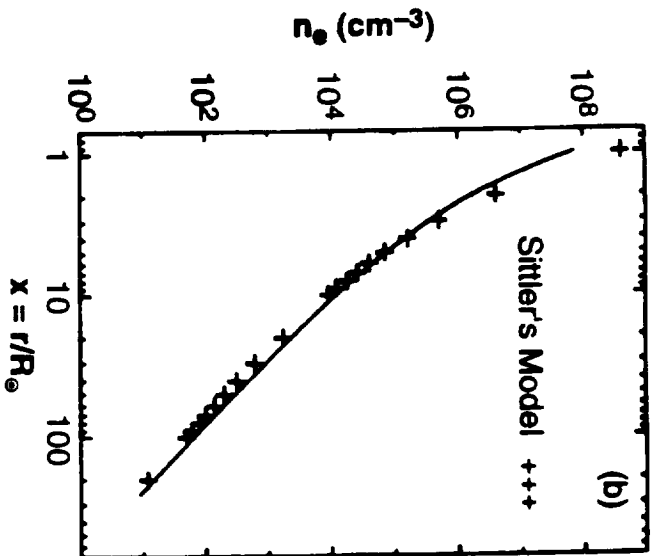
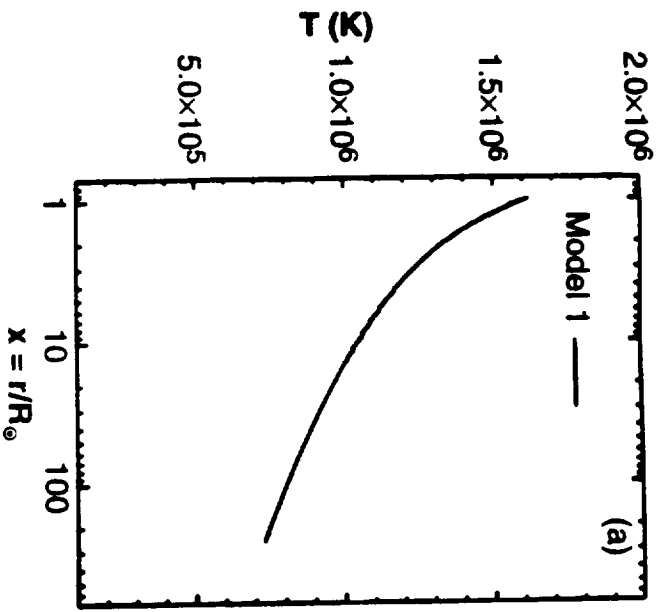


Figure 1

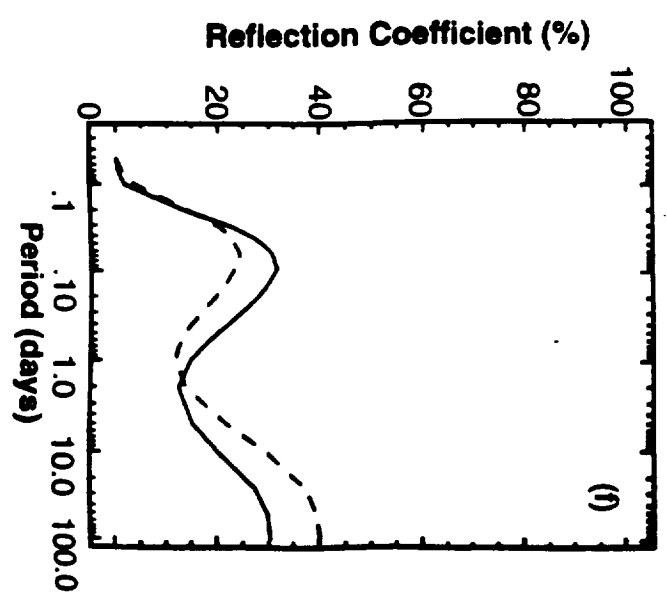
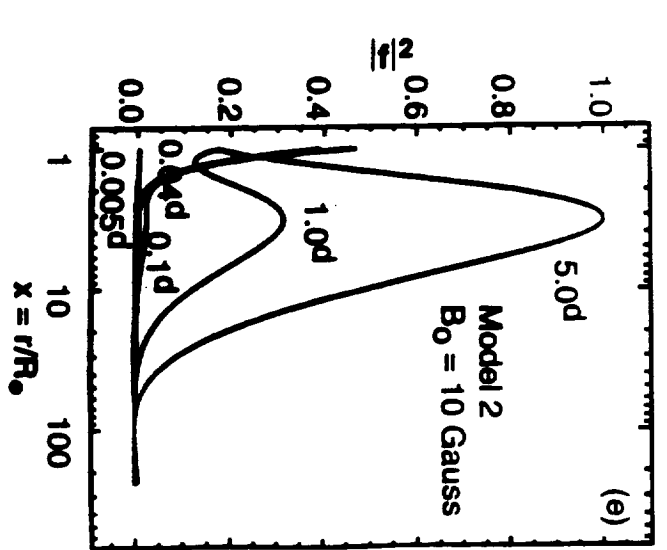
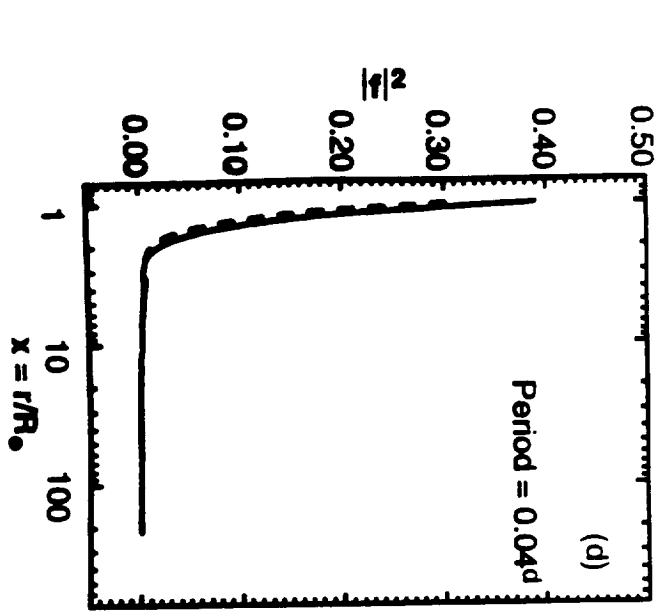
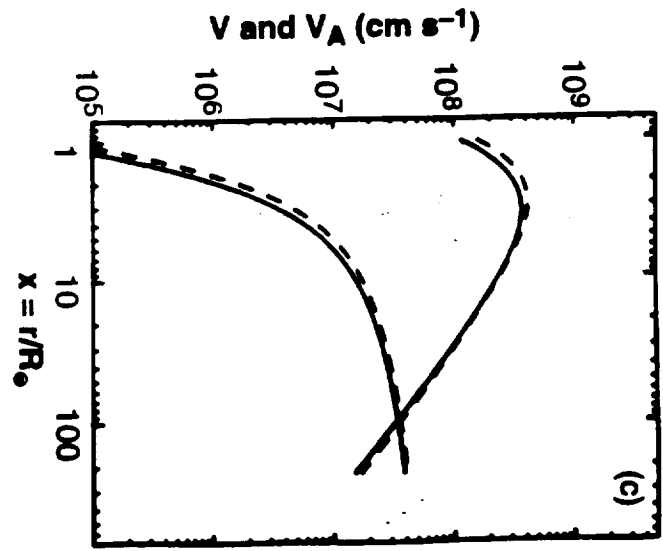
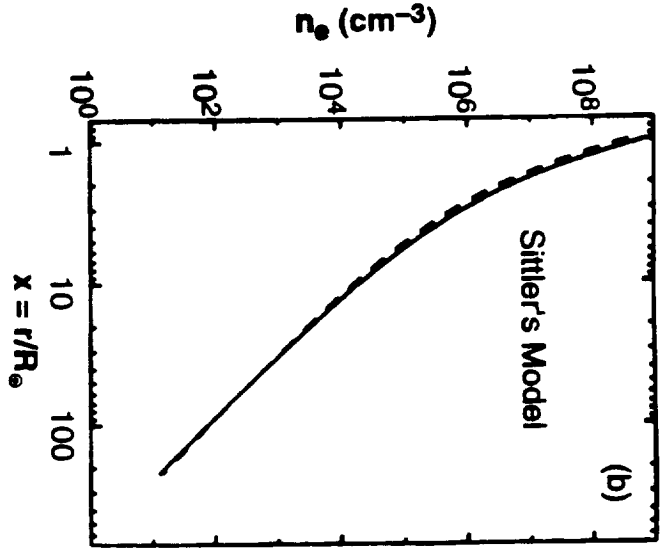
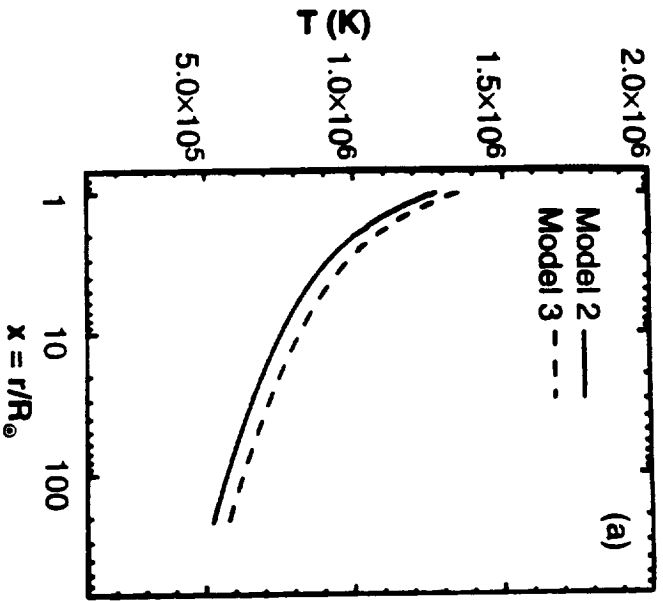


Figure 2

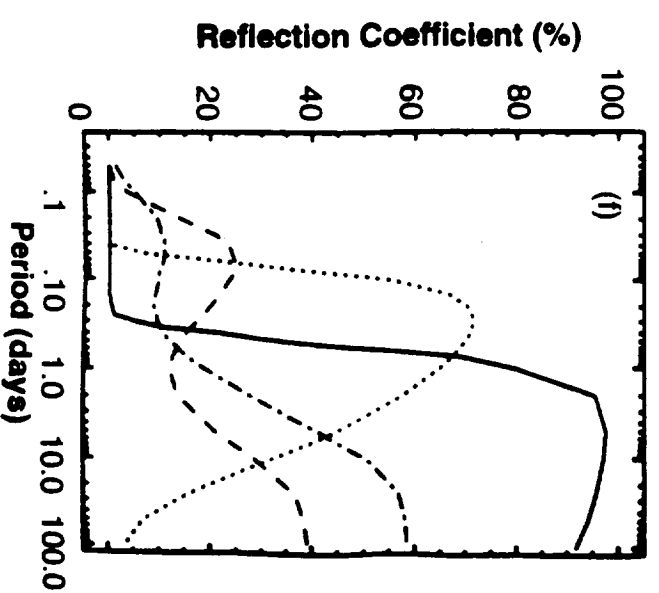
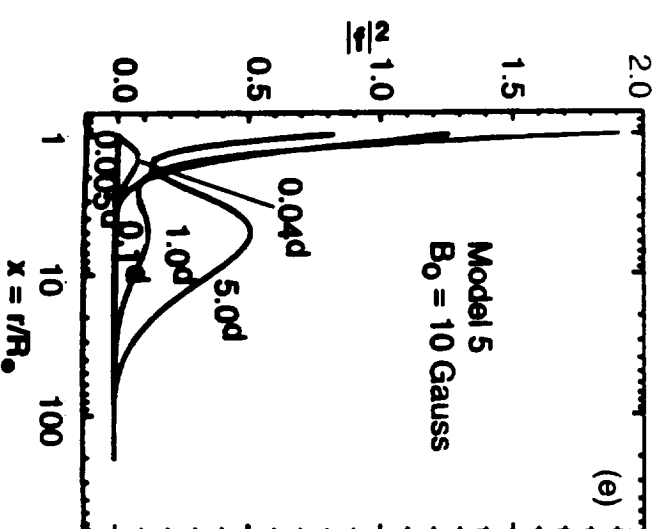
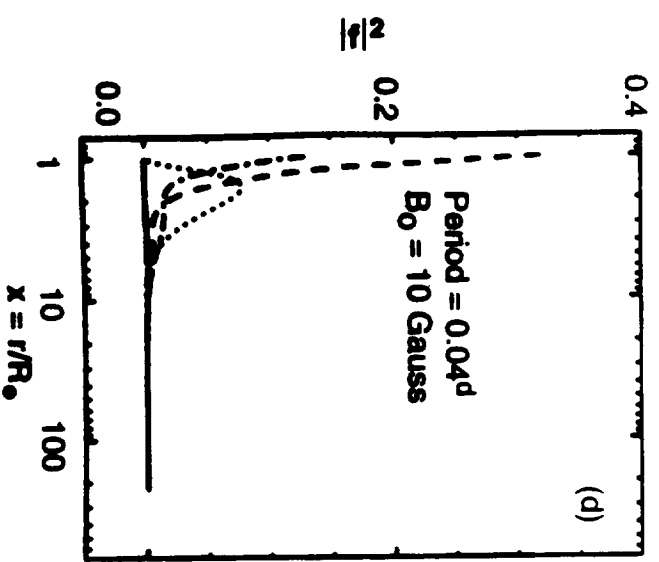
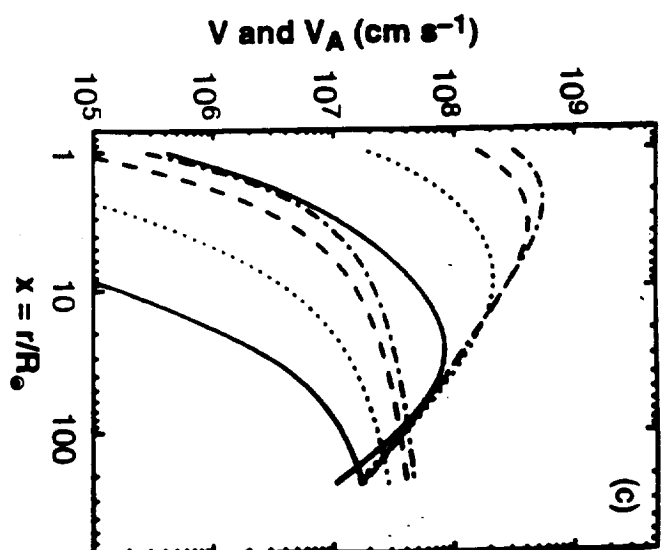
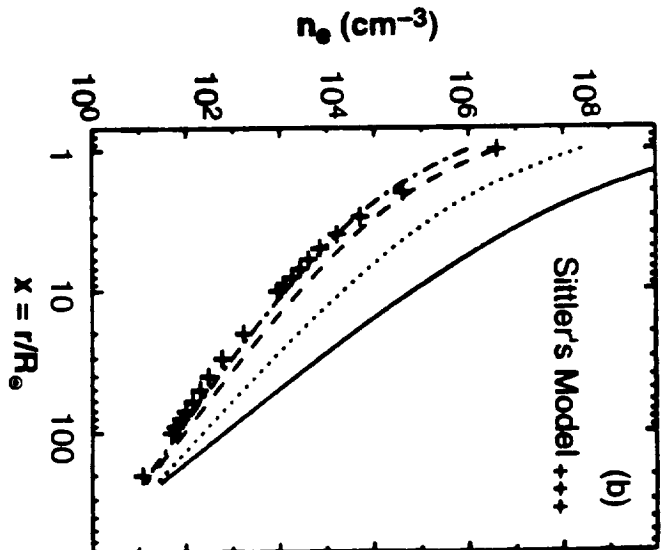
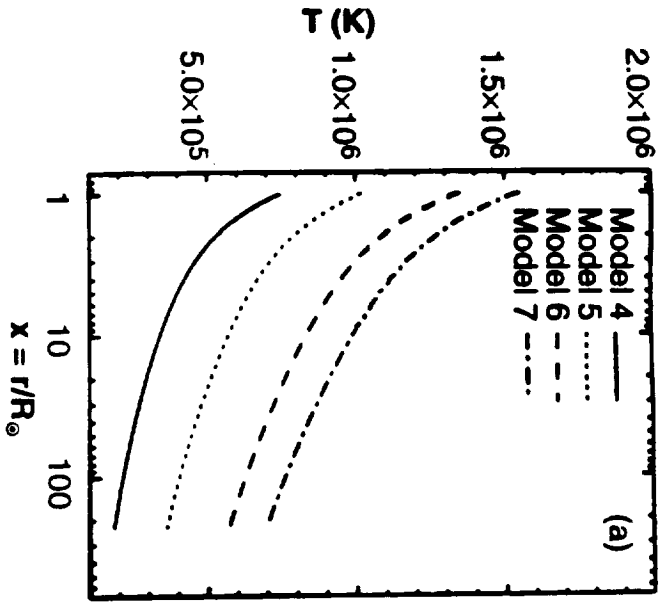


Figure 3

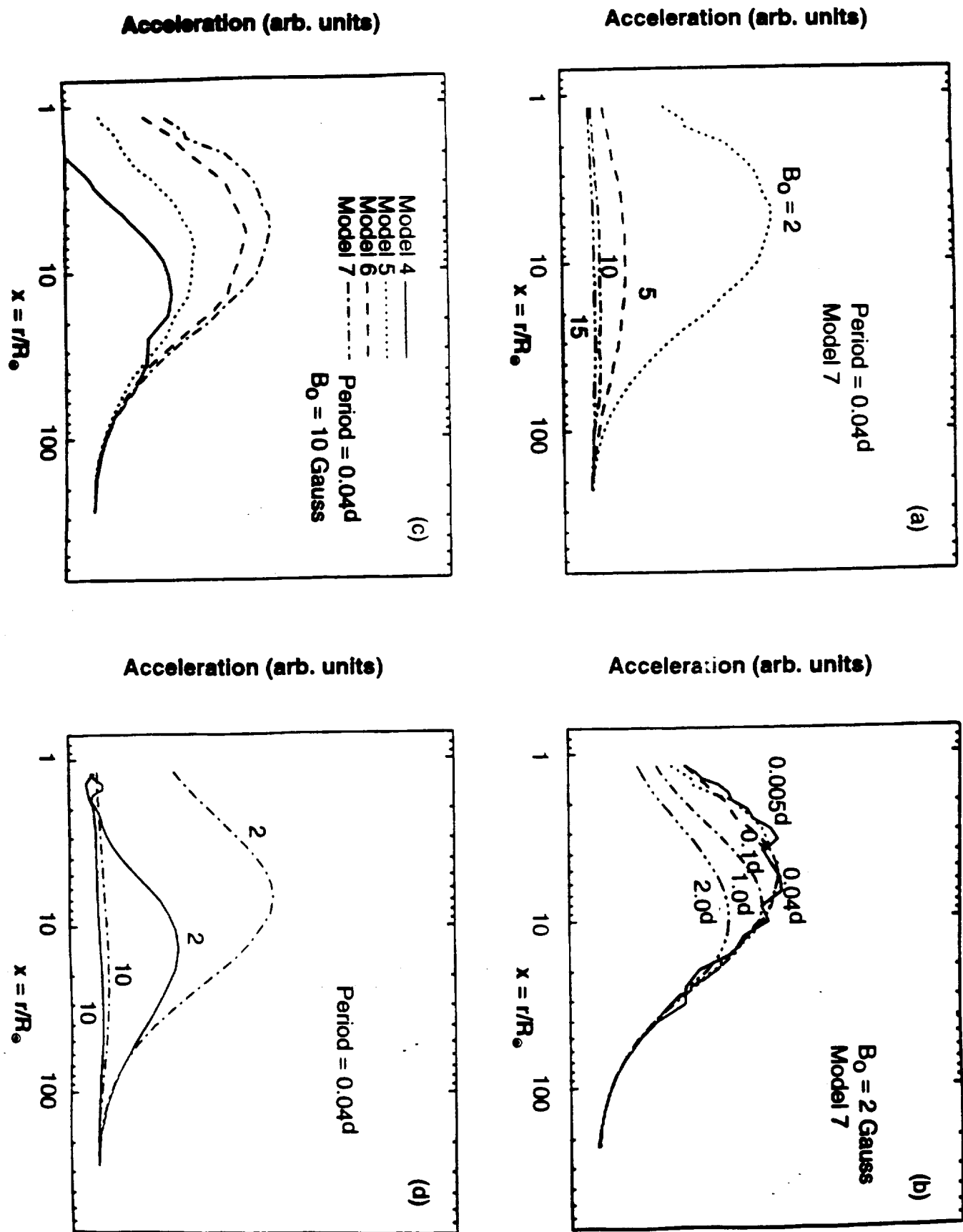


Figure 4

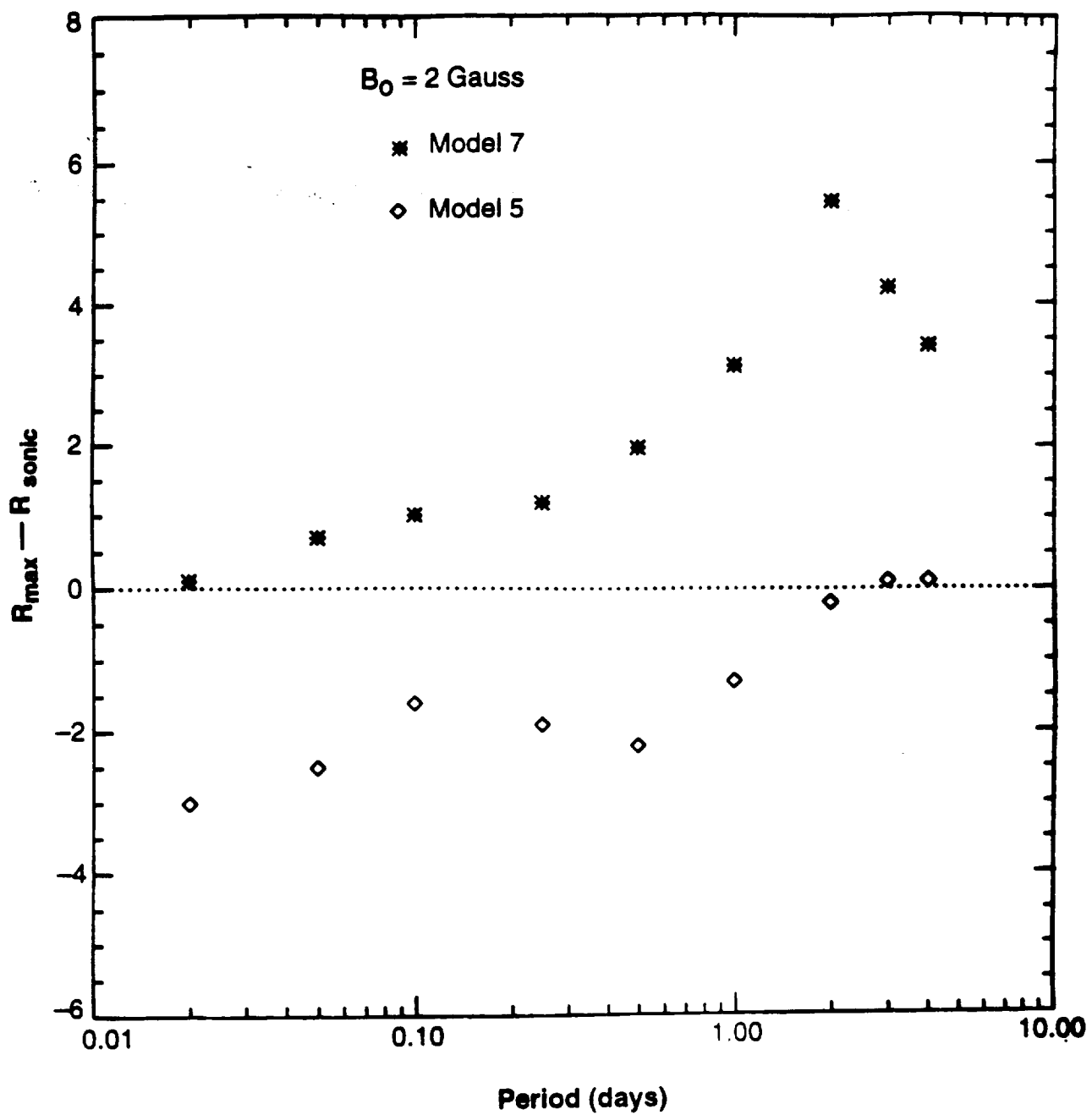


Figure 5